Journal of Inorganic Biochemistry 160 (2016) 189–197

Contents lists available at ScienceDirect

Journal of Inorganic Biochemistry

journal homepage: www.elsevier.com/locate/jinorgbio

Synthesis, characterization and biological evaluation of a ^{67}Ga-labeled (η^6-Tyr)Ru(η^5-Cp) peptide complex with the HAV motif

Zsolt Bihari [a], Filipe Vultos [b], Célia Fernandes [b], Lurdes Gano [b], Isabel Santos [b], João D.G. Correia [b], Péter Buglyó [a,*]

[a] Department of Inorganic and Analytical Chemistry, University of Debrecen, H-4010 Debrecen, P.O.Box 21, Hungary
[b] Centro de Ciências e Tecnologias Nucleares (C^{2}TN), Instituto Superior Técnico, Universidade de Lisboa, Estrada Nacional 10 (km 139,7), 2695-066 Bobadela LRS, Portugal

ARTICLE INFO

Article history:
Received 19 October 2015
Received in revised form 21 January 2016
Accepted 10 February 2016
Available online 11 February 2016

Keywords:
Full sandwich ruthenium complex
Oligopeptide conjugate
Gallium complex
Radiolabeling
HAV sequence
Cadherin

ABSTRACT

Heterobimetallic complexes with the evolutionary, well-preserved, histidyl-alanyl-valinyl (HAV) sequence for cadherin targeting, an organometallic Ru core with anticancer activity and a radioactive moiety for imaging may hold potential as theranostic agents for cancer. Visible-light irradiation of the HAVAY-NH_2 pentapeptide in the presence of [(η^5-Cp)Ru(η^6-naphthalene)]$^+$ resulted in the formation of a full sandwich type complex, (η^6-Tyr-RuCp)-HAVAY-NH_2 in aqueous solution, where the metal ion is connected to the Tyr (Y) unit of the peptide. Conjugation of this complex to 2,2′-(7-(1-carboxy-4-((4-isothiocyanatobenzyl)amino)-4-oxobutyl)-1,4,7-triazonane-1,4-diyl)diacetic acid (NODA-GA) and subsequent metalation of the resulting product with stable (^{nat}Ga) and radioactive (^{67}Ga) isotope yielded ^{nat}Ga/^{67}Ga-NODA-GA-[(η^6-Tyr-RuCp)-HAVAY-NH_2]. The non-radioactive compounds were characterized by NMR spectroscopy and Mass Spectrometry. The cellular uptake and cytotoxicity of the radioactive and non-radioactive complexes, respectively, were evaluated in various human cancer cell lines characterized by different levels of N- or E-cadherins expression. Results from these studies indicate moderate cellular uptake of the radioactive complexes. However, the inhibition of the cell proliferation was not relevant.

1. Introduction

Although the physicochemical properties of metal complexes as potential anticancer drugs can widely be modified by the change of the metal ion and the coordinating ligands, lack of selectivity is still a major drawback for those (mostly square planar Pt(II)) compounds recently used in the treatment of some cancers [1]. Aiming to overcome this issue, these anticancer compounds can be conjugated to targeting biomolecules such as peptides for a specific accumulation in the tumor tissues/cells [2,3]. Indeed, tumor-seeking peptides, are among the most effective targeting moieties known for cellular receptors or drug delivery [2,3].

Endothelial cells form the inner lining of blood vessels and participate in the regulation of the exchange of nutrients and cells between blood and the respective tissues [4]. As nonmalignant cells, they can also be found in solid tumors maintaining a tumor-supporting microenvironment [4]. To preserve the epithelial organization, Ca(II)-dependent cell–cell adhesion and signal transducing integral membrane glycoproteins, cadhedrins, play an important role [5]. Cadherins are expressed in tissue-specific manner as exemplified by the classical cadherins: E-(epithelial), P-(placental) and N-(neural) cadherin [5,6].

N-cadherins have shown to be involved in the formation of blood vessels [7,8]. As adequate blood supply and increased tumor growth are strongly connected to each other, tumor growth is dependent on N-cadherin [9]. It was also demonstrated that in many carcinomas N-cadherin is overexpressed while E-cadherin is down-regulated (cadherin switch) causing tumor cells to resist apoptosis, becoming invasive and metastatic [8,10]. A common structural feature of cadherins is that the first amino-terminal extracellular repeat contains a highly conserved cell adhesion recognition (CAR) sequence, histidyl-alanyl-valinyl (HisAlaVal or HAV), that is crucial for the homophilic cadherin interactions [5,8].

Synthetic oligopeptides, based on the CAR sequence HAV, were shown to inhibit N-cadherin-mediated processes, act as angiogenesis inhibitors or cause apoptosis of various cancer cells [8]. These HAV-containing peptides, as cadherin antagonists, can interfere with cadhedrin mediated cell–cell adhesion and therefore they may also have potential application for the modulation of the intercellular junctions of the biological barrier to improve permeation of drugs via the paracellular pathway [11,12]. Furthermore, in targeted therapy, using an N-cadherin antagonist HAV-peptide, remarkable augmentation of the antitumor effects of chemotherapy was demonstrated to optimize the treatment for melanoma [13].

Organometallic Ru(II) complexes as promising anticancer drug candidates have been the subject of several studies in recent years [14–17]. In particular, full sandwich (η^6-arene)Ru(η^5-Cp*)

* Corresponding author.
E-mail address: buglyo@science.unideb.hu (P. Buglyó).

http://dx.doi.org/10.1016/j.jinorgbio.2016.02.011
0162-0134/

(Cp* = pentamethylcyclopentadienyl anion) type complexes have been shown to exhibit potent antiproliferative effects too [18,19]. Their bioconjugation to tumor-seeking peptides may result in highly selective tumor specific drugs [3,20–22].

Regarding the synthesis of this type of complexes, it was demonstrated that besides the terminal amino or carboxylate groups, phenyl (Phe), phenolic (Tyr) or indol (Trp) aromatic groups of amino acid side chains of the peptides can also be used to obtain organometallic Ru(II) precursors resulting in full sandwich type peptide bioconjugates [23–28]. [(η^5-Cp)Ru(η^6-naphthalene)]PF_6 (Cp = cyclopentadienyl anion) is a readily accessible and air-stable source of the $CpRu^+$ fragment used in complex synthesis and recently was shown to react with the above aromatic side chain groups of peptides in water using visible-light irradiation [25,26,29]. Reaction of the half-sandwich type units (η^6-*p*-cym)Ru(II), (η^5-Cp*)Ru(II), (η^5-Cp*)Rh(III), (η^5-Cp*)Ir(III) (*p*-cym = 1-methyl-4-isopropylbenzene) with aromatic amino acids in the presence of trifluoroacetic acid, resulting in the formation of sandwich complexes with hexa- or pentahapto coordination of the aromatic ring of the amino acid, together with the pH-dependent change in the hapticity of Tyr at high pH in the full sandwich product, is also well documented in the literature [30–32].

Radiolabeled tumor-seeking peptides are widely accepted as clinically useful nuclear tools for molecular imaging or agents for peptide receptor radionuclide therapy, depending on the type of radiation emmitted by the radionuclide [2,33,34]. Among others, the gallium radioisotopes ^{67}Ga ($t_{1/2}$ = 3.26 days, γ-emitter) or ^{68}Ga ($t_{1/2}$ = 68 min, β^+-emitter), for Single Photon Emission Computed Tomography (SPECT) or Positron Emission Tomography (PET) imaging, respectively, complexed by cyclic polyaminocarboxylate ligands, namely 1,4,7-triazacyclononane-1,4,7-triacetic acid (NOTA) derivatives, can efficiently be used for these purposes due to the high thermodynamic stability and the slow ligand exchange processes of the resulting complexes [2,35,36]. The complexing capabilities can be studied using the stable (^{nat}Ga) isotopes.

Based on the above, and taking into account the highly conserved HAV motif of cadherins, we report herein on the synthesis, characterization and preliminary biological evaluation of a heterobimetallic theranostic complex containing the HAV sequence for tumor targeting, a full sandwich type (η^6-Tyr)Ru(η^5-Cp) fragment with potential antitumor activity and a radioactive unit (^{67}Ga-NODA-GA, where NODA-GA = 2,2′-(7-(1-carboxy-4-((4-isothiocyanatobenzyl)amino)-4-oxobutyl)-1,4,7-triazonane-1,4-diyl)diacetic acid) for imaging (Scheme 1).

2. Materials and methods

2.1. Chemicals

[η^5-cyclopentadienyl(η^6-naphthalene)ruthenium(II)](PF_6), NODA-GA were commercial products of the highest purity available (Sigma-Aldrich, CheMatech), and used as received. Rink Amide AM resin, TBTU, Fmoc-protected amino acids were Novabiochem products. N,N-Diisopropyl-ethylamine (DIPEA), trifluoroacetic acid and dimethylformamide (DMF) were purchased from Merck. L-tyrosine was a Reanal (Hungary) product. N-Methylpyrrolidone (NMP), 1-hydroxybenzotriazole hydrate ($HOBt \cdot H_2O$), triisopropylsilane (TIS), 2-methyl-2-butanol and HPLC grade trifluoroacetic acid (TFA) were Sigma-Aldrich products. Dichloromethane, diethyl ether, acetic acid, piperidine, acetic anhydride and acetonitrile were supplied by VWR or Molar.

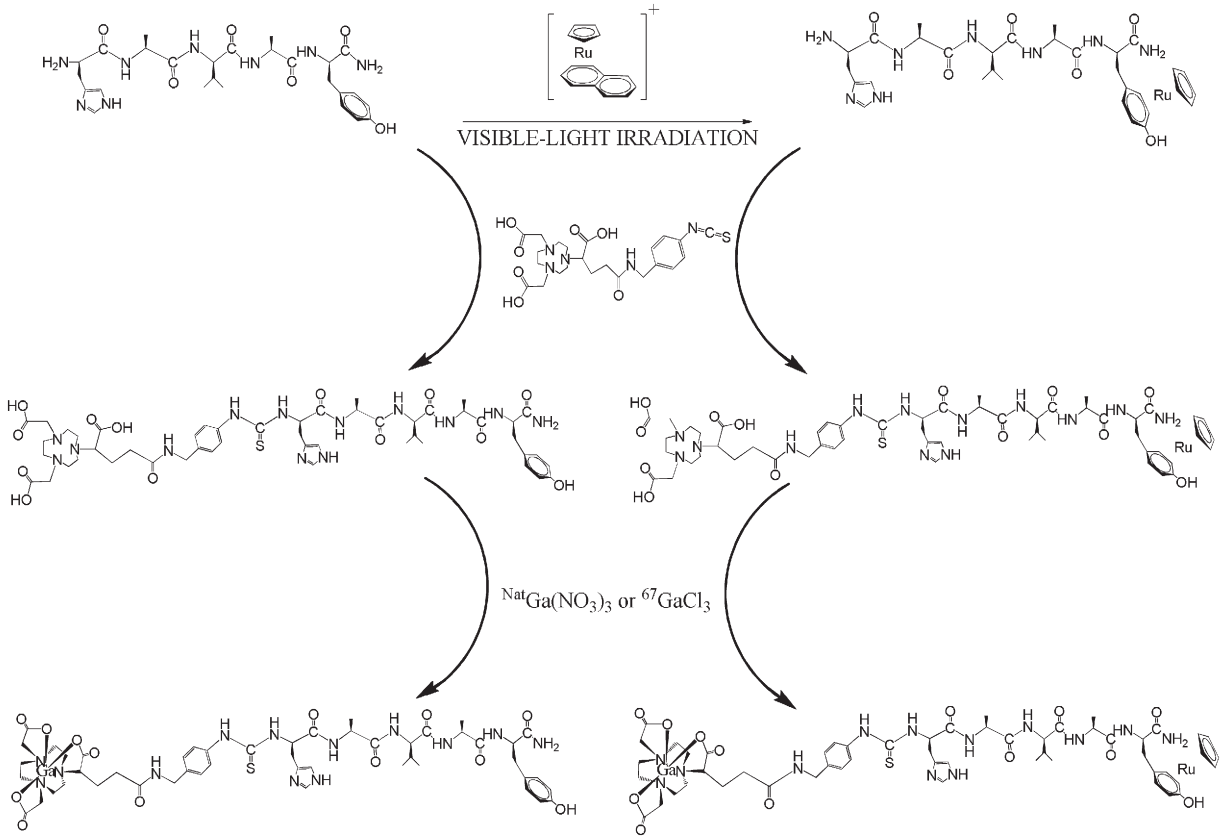

Scheme 1. Synthetic routes for the Ga-NODA-GA-HAVAY-NH_2 and Ga-NODA-GA-(η^6-Tyr-RuCp)-HAVAY-NH_2 peptide complexes.

2.2. Synthesis and physical measurements

2.2.1. [H-HisAlaValAlaTyr-NH_2](CF_3COO)$_2$ (HAVAY-NH_2)

The peptide was synthesized by solid phase peptide synthesis in a microwave-assisted Liberty 1 Peptide Synthesizer (CEM, Matthews, NC), using the TBTU/HOBt/DIPEA activation strategy on Rink Amide AM resin (substitution 0.71 mmol·g^{-1}, 0.25 mmol·g scale, 352 mg of resin). Removal of the Fmoc group was carried out by means of 20% piperidine/0.1 M HOBt·H_2O in DMF at 75 °C with 35 watts microwave power for 180 s. 0.5 M HOBt·H_2O/0.5 M TBTU in DMF and 2 M DIPEA in NMP were used for coupling at 75 °C with 25 watts microwave power, for 300 s, adding 4 times excess of amino acids. The N-terminal Fmoc group was removed as described before. Cleaving from the resin and removal of the side chain protective groups were carried out by treatment with a mixture containing TFA/TIS/H_2O/DODT (94/2.5/2.5/1 v/v %) at room temperature for 1.5 h. After cleaving the solution, the free peptide was separated from the resin by filtration. Cold Et_2O was used to precipitate the crude peptide from the solution and to wash from the contaminants of the reagents of the synthesis and cleaving agents. After filtering, the product was dried under argon, redissolved in water and lyophilized. Purity of the peptide (>95%) was checked by analytical RP-HPLC. R_t = 4.47 min using HPLC (system I). Yield: 145.5 mg (74%). ^1H *NMR* (D_2O, *400 MHz*): δ [*ppm*] 8.70 (1H, s, His-C*Hε*); 7.44 (1H, s, His-C*Hδ*); 7.14 (2H, d, J = 8.4 Hz, Tyr-C*Hδ*); 6.83 (2H, d, J = 8.4 Hz, Tyr-C*Hε*); 4.50 (1H, dd, J = 7.9 Hz and 6.7 Hz, Tyr-C*Hα*); 4.44 (1H, q, J = 7.2 Hz, Ala-C*Hα*); 4.36–4.28 (overlapping: 1H, q, Ala-C*Hα* and 1H, dd, His-C*Hα*); 4.07 (1H, d, J = 7.5 Hz, Val-C*Hα*); 3.48–3.34 (2H, m, His-C*Hβ*); 3.00 (2H, m, J = 22.4 Hz, 14.0 Hz and 7.4 Hz, Tyr-C*Hβ*); 1.99 (1H, m, J = 13.8 Hz and 6.8 Hz, Val-C*Hβ*); 1.39 (3H, d, J = 7.2 Hz, Ala-C*Hβ*); 1.32 (3H, d, J = 7.1 Hz, Ala-C*Hβ*); 0.89 (6H, dd, J = 23.8 Hz and 6.7 Hz Val-C*Hβ*). ^{13}C *NMR* (D_2O, *100.6 MHz*): δ [*ppm*] 175.5, 174.7, 174.1, 172.7, 167.6 (5C, CO); 154.4 (1C, Tyr-Cζ); 134.4 (1C, His-Cε); 130.5 (2C, Tyr-Cδ); 128.1 (1C, His-Cγ); 125.5 (1C, Tyr-Cγ); 118.7 (1C, His-Cδ); 115.4 (2C, Tyr-Cε); 59.5 (1C, Val-Cα); 54.7 (1C, Tyr-Cα); 51.6 (1C, His-Cα); 49.6 (1C, Ala-Cα); 49.2 (1C, Ala-Cα); 36.2 (1C, Tyr-Cβ), 30.2 (1C, Val-Cβ); 26.0 (1C, His-Cβ); 18.3 (1C, Val-Cγ); 17.7 (1C, Val-Cγ); 16.6 (1C, Ala-Cβ); 16.5 (1C, Ala-Cβ). *ESI-MS* (*pos.*) *m/z*: 559.293 [M – 2 CF_3COO – H]$^+$, calc. for $C_{26}H_{39}N_8O_6$: 559.299; 581.275 [M − 2 CF_3COO – 2H + Na]$^+$, calc. for $C_{26}H_{38}N_8O_6Na$: 581.281.

2.2.2. [(η^6-Tyr-RuCp)-HAVAY-NH_2](CF_3COO)$_3$

[η^5-cyclopentadienyl(η^6-naphthalene)ruthenium(II)](PF_6) (26.34 mg, 60 μmol) and HAVAY-NH_2 (34.63 mg, 44 μmol) were dissolved in D_2O (6.5 ml). Visible-light irradiation was performed by a halogen lamp (500 W, 9 k lumen) at ca. 35 °C. The reaction mixture was stirred for 4 days. Color of the solution changed from yellow to brownish and free naphthalene as solid appeared. After complete reaction (monitored by ^1H NMR) the solution with the full sandwich ruthenium(II) peptide conjugate was lyophilized and the naphthalene formed was removed in a vacuum-line. The crude product was redissolved in distilled water and purified using HPLC (system II) (purity >95%). R_t = 5.17 min. ^1H *NMR* (D_2O, *400 MHz*, *low-field region*): δ [*ppm*] 8.75 (1H, s, His-C*Hε*); 7.48 (1H, s, His-C*Hδ*); 6.14 (2H, m, (η^6-Tyr-C*Hδ*)Ru(η^5-Cp); 6.03 (2H, m, (η^6-Tyr-C*Hε*)Ru(η^5-Cp); 5.34 (5H, s, (η^6-Tyr)Ru(η^5-Cp-H^{Ar})). ^{13}C *NMR* (D_2O, *100.6 MHz*): δ [*ppm*] 134.4 (1C, His-*Cε*); 118.7 (1C, His-*Cδ*); 85.5 (2C, (η^6-Tyr-*Cε*)Ru(η^5-Cp); 84.9 (2C, (η^6-Tyr-*Cδ*)Ru(η^5-Cp), 80.2 (5C, (η^6-Tyr)Ru(η^5-Cp-C^{Ar}). *ESI-MS* (*pos.*) *m/z*: 725.225 [M − 3 CF_3COO − 2 H]$^+$, calc. for $C_{31}H_{43}N_8O_6Ru$: 725.235; 363.112 [M − 3 CF_3COO − H]$^{2+}$, calc. for $C_{31}H_{44}N_8O_6Ru$: 363.121.

2.2.3. [NODA-GA-HAVAY-NH_2](CH_3COO)$_2$

To a 25 ml round-bottom flask containing N-terminally free HAVAY-NH_2 pentapeptide (4.2 mg, 5.3 μmol) and DIPEA (20 μl) in DMF (0.8 ml) was added NODA-GA (2.8 mg, 5.4 μmol). The reaction mixture was stirred at room temperature for 4 h and the reaction was quenched with AcOH (30 μl in 2.0 ml of water). The crude product was purified with a semi-preparative HPLC (III). The fractions collected were evaporated, redissolved in water and lyophilised (purity >95% by HPLC (system II), R_t = 10.19 min). ^1H *NMR* (D_2O, *400 MHz*): δ [*ppm*] 8.72 (1H, s, His-C*Hε*); 7.44 (2H, d, J = 8.2 Hz, NODA-Ar*H*); 7.40 (1H, s, His-C*Hδ*); 7.15 (2H, d, J = 8.4 Hz, Tyr-C*Hδ*); 7.02 (2H, d, J = 8.1 Hz, NODA-Bn*H*); 6.83 (2H, d, J = 8.5 Hz, Tyr-C*Hε*); 4.50 (1H, dd, J = 8.3 Hz and 6.4 Hz, Tyr-C*Hα*); 4.42 (1H, q, J = 15.6 Hz, His-C*Hα*); 4.31 (1H, q, J = 7.1 Hz, Ala-C*Hα*); 4.12 (1H, dd, J = 7.2 Hz, Ala-C*Hα*); 4.08 (1H, d, J = 7.5 Hz, Val-C*Hα*); 3.81–2.50 (overlapping signals); 2.27–2.00 (overlapping: *2×2H*, *m*, NODA-CH_2); 1.96 (1H, m, J = 13.7 Hz and 6.9 Hz, Val-C*Hβ*); 1.50 (3H, d, J = 7.1 Hz, Ala-C*Hβ*); 1.31 (3H, d, J = 7.2 Hz, Ala-C*Hβ*); 0.87 (6H, dd, J = 20.7 Hz and 6.8 Hz Val-C*Hβ*). *ESI-MS* (*pos.*) *m/z*: 1080.567 [M − 2 CH_3COO − H]$^+$, calc. for $C_{49}H_{70}N_{13}O_{13}S$: 1080.494; 541.122 [M − 2 CH_3COO]$^{2+}$, calc. for $C_{49}H_{71}N_{13}O_{13}S$: 541.252.

2.2.4. [NODA-GA-(η^6-Tyr-RuCp)-HAVAY-NH_2](CH_3COO)$_3$

To a 25 ml round-bottom flask containing (η^6-Tyr-RuCp)-HAVAY-NH_2 complex (4.8 mg, 4.5 μmol) and DIPEA (20 μl) in DMF (0.8 ml) was added NODA-GA (2.8 mg, 5.4 μmol). The reaction mixture was stirred at room temperature for 6 h and the reaction was quenched with AcOH (30 μl in 2.0 ml of water). The crude product was purified by preparative HPLC (system III). The fractions collected were evaporated, redissolved in water and lyophilised. The purity of the product was >95% by HPLC (system II), R_t = 7.98 min. ^1H *NMR* (D_2O, *400 MHz*, *low-field region*): δ [*ppm*] 8.75 (1H, s, His-C*Hε*); overlapping (2H, d, NODA-Ar*H*; 1H, s, His-C*Hδ*); 7.06 (2H, d, NODA-Bn*H*); 6.14 (2H, m, (η^6-Tyr-C*Hδ*)Ru(η^5-Cp); 6.06 (2H, m, (η^6-Tyr-C*Hε*)Ru(η^5-Cp); 5.35 (5H, s, (η^6-Tyr)Ru(η^5-Cp-H^{Ar}). *ESI-MS* (*pos.*) *m/z*: 623.714 [M − 3 CH_3COO − H]$^{2+}$, calc. for [$C_{54}H_{75}N_{13}O_{13}RuS$]$^{2+}$: 623.719; 1246.318 [M − 3 CH_3COO − 2H]$^+$, calc. for $C_{54}H_{74}N_{13}O_{13}RuS$: 1246.429; *ESI-MS* (*neg.*) *m/z*: 1244.468 [M − 3 CH_3COO − 4H]$^-$, calc. for $C_{54}H_{72}N_{13}O_{13}RuS$: 1244.417.

2.2.5. [Ga-NODA-GA-HAVAY-NH_2](CH_3COO)

To a 25 ml round-bottom flask containing NODA-GA-HAVAY-NH_2 (1.8 mg, 1.5 μmol) dissolved in acetate buffer pH 4.0 (0.8 ml) was added $Ga(NO_3)_3$·H_2O (2.0 mg, 7.2 μmol). The reaction mixture was stirred at room temperature for 2 h and was purified by HPLC (system III). The fractions collected were evaporated, redissolved in water and lyophilised. The purity of the product was >95% by analytical HPLC (system II). R_t = 7.14 min. ^1H *NMR* (D_2O, *400 MHz*, *low-field region*): δ [*ppm*] 8.44 (1H, s, His-C*Hε*); 7.36 (2H, d, J = 8.2 Hz, NODA-Ar*H*); 7.34 (1H, s, His-C*Hδ*); 7.08 (2H, d, J = 8.4 Hz, Tyr-C*Hδ*); 6.97 (2H, d, J = 8.1 Hz, NODA-Bn*H*); 6.76 (2H, d, J = 8.5 Hz, Tyr-C*Hε*). ^{71}Ga *NMR* (D_2O, *122 MHz at 313.15 K*): δ [*ppm*] 164.7 (1Ga, s, $\Delta\omega_{½}$ = 517 Hz), 0 (1Ga, s, [$Ga(H_2O)_6$]$^{3+}$); *ESI-MS* (*pos.*) *m/z*: 1146.7 [M − CH_3COO]$^+$, calc. for $C_{49}H_{67}GaN_{13}O_{13}S$: 1146.396.

2.2.6. [Ga-NODA-GA-(η^6-Tyr-RuCp)-HAVAY-NH_2](CH_3COO)$_2$

To a 25 ml round-bottom flask containing NODA-GA-(η^6-Tyr-RuCp)-HAVAY-NH_2 (0.7 mg, 0.5 μmol) in acetate buffer pH 4.0 (0.8 ml) was added $Ga(NO_3)_3$·H_2O (2.0 mg, 7.2 μmol). The reaction mixture was stirred at room temperature for 4 h. The reaction mixture was purified by preparative HPLC (system III). The fractions collected were evaporated, redissolved in water and lyophilised. The purity of the product was >95% by analytical HPLC (system II). R_t = 5.84 min. ^1H *NMR* (D_2O, *400 MHz*, *low-field region*): δ [*ppm*] 8.65 (1H, s, His-C*Hε*); 7.31 (overlapping 2H, d, NODA-Ar*H* and 1H, s, His-C*Hδ*); 6.98 (2H, d, NODA-Bn*H*); 6.13 (2H, m, (η^6-Tyr-C*Hδ*)Ru(η^5-Cp); 6.05 (2H, m, (η^6-Tyr-C*Hε*)Ru(η^5-Cp); 5.34 (5H, s, (η^6-Tyr)Ru(η^5-Cp-H^{Ar}). ^{71}Ga *NMR* (D_2O, *122 MHz at 313.15 K*): δ [*ppm*] 164.5 (1Ga, s, $\Delta\omega_{½}$ = 565 Hz), 0 (1Ga, s, [$Ga(H_2O)_6$]$^{3+}$). *ESI-MS* (*pos.*) *m/z*: 656.665 [M − 2 CH_3COO]$^{2+}$, calc. for

$[C_{54}H_{72}GaN_{13}O_{13}RuS]^{2+}$: 656.670; 1312.230 $[M - 2\,CH_3COO - H]^+$, calc. for $C_{54}H_{71}GaN_{13}O_{13}RuS$: 1312.332.

2.2.7. Radiosynthesis of ^{67}Ga-labeled peptide conjugates

^{67}Ga is a gamma emitter ($t_{1/2}$ = 3.25 days; E = 93 keV (35.7%), 185 keV (19.7%), 300 keV (16.0%)). Therefore, all manipulations were carried out under the supervision of well experienced researchers in specially equipped licensed laboratories in compliance with the radiation protection and safety program of the C^{2}TN.

Gallium-67 citrate was a gift from the nuclear medicine service of Hospital de Santa Maria (Lisbon, Portugal). Gallium-67 chloride ($^{67}GaCl_3$) was prepared from Gallium-67 citrate as described in the literature [37]. $^{67}GaCl_3$ (150 to 300 μCi) was added to the conjugates (5.0×10^{-5} M) in 0.3 ml of 400 mM sodium acetate buffer pH 5.0 and incubated at room temperature for 1 h. The reaction mixture was purified using a Sep-pak C18 cartridge to separate the uncomplexed radioactive gallium (eluted with water) from the ^{67}Ga-labeled peptide conjugates (eluted with ethanol). The radiochemical purity was determined by HPLC analysis (system IV). R_t = 11.6 min (^{67}Ga-NODA-GA-HAVAY-NH_2), 11.5 min (^{67}Ga-NODA-GA-(η^6-Tyr-RuCp)-HAVAY-NH_2).

2.3. Solution studies

2.3.1. pH-potentiometry

For solution studies doubly deionized and ultra-filtered water was obtained from a Milli-Q RG (Millipore) water purification system. pH-potentiometric measurements were carried out at an ionic strength of 0.20 M KNO_3 and at 25.0 ± 0.1 °C. Carbonate-free KOH solutions of known concentrations (*ca.* 0.2 M) were used as titrant. HNO_3 stock solution (*ca.* 0.2 M) was prepared from concentrated nitric acid and the exact concentration was determined by potentiometric titrations using the Gran's method [38]. A Mettler Toledo T50 titrator equipped with a Metrohm double junction electrode (type 6.0255.100) was used for the pH-metric measurements. The electrode system was calibrated according to Irving et al. [39], the pH-metric readings could therefore be converted into hydrogen ion concentration. The water ionization constant, pK_w, was 13.76 ± 0.01. Automatic titrations with a maximum waiting time of 2.5 min in every step were performed in the pH range 2.0–11.0 using samples of 4.00 ml. The samples were in all cases completely deoxygenated by bubbling purified argon for *ca.* 20 min before the measurements. Calculation of the protonation constants of the HAVAY-NH_2 was performed with the aid of the SUPERQUAD computer program [40].

2.3.2. High-performance liquid chromatography

HPLC (*system I*): Jasco analytical HPLC instrument, equipped with a Jasco MD-2010 plus multiwavelength detector. The analyses were performed on a Vyday C18 chromatographic column (250 × 4.6 mm, 300 Å pore size, 5 μm particle size) by eluting 10% of solvent A (0.1% TFA in water) and 90% of solvent B (0.1% TFA in ACN) at flow rate of 1 ml/min monitoring the absorbance at 222 nm. Method: 30 min 90% A and 10% B (isocratic).

HPLC (*system II*): Perkin-Elmer Series 200 analytical HPLC instrument, equipped with a UV/Vis detector (LC 290). The analyses were performed on a Supelco Analytical Discovery BIO WidePore C18_5 column (250 × 4.6 mm, 300 Å pore size, 5 μm particle size) by eluting A solvent (0.1% TFA in water) and B solvent (0.1% TFA in ACN) at flow rate of 1 ml/min monitoring the absorbance at 254 nm. Method: 10 min 90% A and 10% B (isocratic), 20 min 20% A and 80% B (gradient).

HPLC (*system III*): Waters semi-preparative HPLC instrument (Waters 2535 Quaternary Gradient Module), equipped with a diode array detector (Waters 2996). The analyses were performed on a Supelco Analytical Discovery BIO WidePore C18_5 column (250 × 10 mm, 300 Å pore size, 10 μm particle size) by eluting A solvent (0.1% TFA in water) and B solvent (0.1% TFA in ACN) at flow rate of 2 ml/min monitoring the absorbance at 254 and 280 nm. Method: 2 min 85% A and 15% B (isocratic), 20 min 0% A and 100% B (gradient), 3 min 0% A and 100% B (isocratic), 2 min 85% A and 15% B (gradient), 3 min 85% A and 15% B (isocratic).

HPLC (*system IV*): Perkin-Elmer LC 200 HPLC coupled to a LC 290 UV/Vis detector and to a Berthold LB-507 A radiometric detector. The analyses were performed on a EC 250/4 Nucleosil 100-10 C18 (REF: 720023.40). (250 × 4 mm, 300 Å pore size, 5 μm particle size) by eluting A solvent (0.1% TFA in water) and B solvent (0.1% TFA in ACN) at flow rate of 1 ml/min monitoring the absorbance at 254 nm. Method: 2 min 95% A and 5% B (isocratic), 20 min 0% A and 100% B (gradient), 3 min 0% A and 100% B (isocratic), 2 min 95% A and 5% B (gradient), 3 min 95% A and 5% B (isocratic).

2.3.3. NMR spectroscopy

The NMR spectra (^{1}H, ^{13}C, ^{1}H–^{1}H COSY, ^{1}H–^{13}C HSQC, ^{71}Ga) were recorded on a Bruker Avance DRX 400 MHz FT-NMR instrument. Chemical shifts are reported in ppm (δ_H) from sodium 3-(trimethylsilyl)-propionate (TSP) as internal reference. NMR studies were carried out in D_2O (99.8%). pH* was set up with NaOD or DNO_3 in D_2O. pH* values (direct pH-meter readings in a D_2O solution of a pH-meter calibrated in H_2O according to Irving et al. [39]) were converted to pH values using the following equation: pH = pH* + 0.40 [41]. Calculation of the protonation constant of (η^6-L-Tyr-Ru(η^5-Cp) complex was carried out with the aid of the Scientist program [42].

2.3.3.1. Formation of $[(\eta^6\text{-}(HO\text{-}C_6H_4\text{-}CH(NH_3)COO)Ru(\eta^5\text{-}Cp)]^+$ in solution. [η^5-cyclopentadienyl(η^6-naphthalene)ruthenium(II)](PF_6) (9.88 mg, 20 μmol or 5.09 mg, 10 μmol) and L-tyrosine (3.66 mg, 20 μmol or 1.89 mg, 10 μmol) were dissolved in D_2O (2.0 ml) or in H_2O (1.0 ml), respectively.

Visible-light irradiation was performed by a halogen lamp (500 W, 9 k lumen) at ca. 31 °C, while stirring for 1 day in both samples. The solutions changed from yellow to brownish and free naphthalene appeared in the vessels. The reaction was monitored by using ^{1}H NMR techniques. *^{1}H NMR* (*D_2O, 400 MHz, pH = 3.23*): δ [*ppm*] 6.17–6.08 (4×1H, m, L-Tyr-*$H^{Ar}\delta$* and L-Tyr-*$H^{Ar}\varepsilon$*); 5.34 (5H, s, (η^5-L-Tyr)Ru(η^5-Cp-*H^{Ar}*); 3.95 (1H, m, L-Tyr-C*Hα*); 2.95 (2H, m, L-Tyr-C*Hβ*). *^{13}C NMR* (*D_2O, 100.6 MHz*): δ [*ppm*] not observed (1C, −*C*(=O)O); 131.76 (1C, L-Tyr-Cζ, C-OH); 95.16 (1C, L-Tyr-Cγ); 85.6, 85.2 (2C, L-Tyr-C*δ*); 80.6 (5C, Cp-C); 75.1, 74.9 (2C, L-Tyr-C*ε*); 55.4 (1C, L-Tyr-C*α*); 34.9 (1C, L-Tyr-C*β*). *ESI-MS* (*pos.*) *m/z*: 348.006 $[M - H]^+$, calc. for $C_{14}H_{16}NO_3Ru$: 348.017.

2.3.3.2. Formation of $[(\eta^5\text{-}(O\text{-}C_6H_4\text{-}CH(NH_2)COO)Ru(\eta^5\text{-}Cp]^-$ in solution. In the NMR sample of $[(\eta^6\text{-}(HO\text{-}C_6H_4\text{-}CH(NH_3)COO)Ru(\eta^5\text{-}Cp)]^+$ the pH was increased with NaOD to form the η^5-oxohexadienyl coordinating L-tyrosine in the full sandwich type $[(\eta^5\text{-}(O\text{-}C_6H_4\text{-}CH(NH_2)COO)Ru(\eta^5\text{-}Cp)]^-$ complex. *^{1}H NMR* (*D_2O, 400 MHz, pH = 9.73*): δ [*ppm*] 5.77 (2×1H, m, L-Tyr-*$H^{Ar}\delta$*); 5.50 (2×1H, m, L-Tyr-*$H^{Ar}\varepsilon$*); 5.11 (5H, s, (η^5-L-Tyr)Ru(η^5-Cp-*H^{Ar}*); 3.51 (1H, m, L-Tyr-C*Hα*); 2.64 (2H, m, J = 20.8 Hz, 13.9 Hz and 6.4 Hz, L-Tyr-C*Hβ*). *^{13}C NMR* (*D_2O, 100.6 MHz*): δ [*ppm*] not observed (1C, −*C*(=O)O); 146.1 (1C, L-Tyr-Cζ); 92.7 (1C, L-Tyr-Cγ); 85.6 (2C, L-Tyr-C*δ*); 78.2 (5C, Cp-*C*); 75.4 (2C, L-Tyr-C*ε*); 57.3 (1C, L-Tyr-C*α*); 38.7 (1C, L-Tyr-C*β*). *ESI-MS* (*neg.*) *m/z*: 346.001 $[M - 3H]^-$, calc. for $C_{14}H_{14}NO_3Ru$: 346.002.

2.3.4. Mass spectrometry

ESI-TOF MS analysis in the positive or negative mode was carried out on a Bruker micrOTOF$_Q$ instrument. The measurements were performed in water, acetonitrile or methanol. Temperature of drying gas (N_2) was 180 °C. The pressure of the nebulizating gas (N_2) was 0.3 bar. The flow rate was 3 μl/min. The spectra were accumulated and recorded by a digitalizer at a sampling rate of 2 GHz. DataAnalysis (version 3.4) was used for the calculation.

Table 1
Downfield (Cp) or upfield (Tyr) shifts of the hydrogen atoms and upfield shifts of the carbon atoms of the Tyr, as a result of the formation of (η^5-Cp)Ru(η^6-Tyr) type full sandwich complex.

Cp-H^{Ar}	(η^5-Cp)Ru(η^6-Naphthalene)	(η^6-Tyr-RuCp)-HAVAY-NH_2	Δδ (ppm)
Hα	5.02	5.34	+0.32
Tyr-H^{Ar}	HAVAY-NH_2	(η^6-Tyr-RuCp)-HAVAY-NH_2	Δδ (ppm)
Hδ	7.14	6.14	−1.01
Hε	6.83	6.08	−0.75
Tyr-C^{Ar}	HAVAY-NH_2	(η^6-Tyr-RuCp)-HAVAY-NH_2	Δδ (ppm)
Cδ	130.5	85.5	−45.0
Cε	115.4	84.9	−30.5

2.4. In vitro studies

2.4.1. Cell culture

MCF-7 and MDA-MB-231 breast adenocarcinoma and A375 melanoma cells of human origin (Table 2) [11,43,44] were grown in Dulbecco's modified Eagle's medium containing GlutaMax I supplemented with 10% heat-inactivated fetal bovine serum (FBS) and 1% penicillin/streptomycin antibiotic solution. PC-3 human prostate cancer cells (Table 2) [43] were grown in RPMI 1640 medium supplemented with 10% FBS and 1% antibiotic solution. Cells were cultured in a humidified 5% CO_2 atmosphere, at 37 °C.

2.4.2. Cellular uptake studies

Cellular uptake studies of the ^{67}Ga complexes were performed using MCF-7, MDA-MB-231, PC-3 and A375 cell lines. Cells were seeded at a density of 2×10^5 cells/0.5 ml per well in 24-well plate in culture medium and allowed to attach overnight. After 24 h, the medium was removed and cells were treated with fresh medium containing approximately 4×10^5 cpm/0.5 ml of each ^{67}Ga complex and incubated under a humidified 5% CO_2 atmosphere, at 37 °C. After 5, 15, 30, 60, 120 and 240 minutes incubation period the cells were washed twice with cold PBS, lysed with 0.1 M NaOH and the cellular extracts were measured for radioactivity. Each experiment was performed in duplicate with each point determined in four replicates. Cellular uptake data were expressed as an average plus the standard deviation of % of total per million cells.

2.4.3. Internalization studies

Internalization assays were performed by incubation of 2×10^5 cells with 4×10^5 cpm/0.5 ml of each ^{67}Ga complex per well in 24 multiplate for a period of 5 min to 4 h as described above. Incubation was finished by washing the cells with ice-cold assay medium. Cell surface bound radioactivity was removed by two steps of acid wash with 50 mM glycine, HCl/100 mM NaCl, pH 2.8 at room temperature for 4 min. The pH was neutralized with cold PBS with 0.2% BSA, and subsequently the cells were lysed by 10 min incubation with 1 M NaOH at 37 °C. The radioactivity associated to each fraction was measured in a gamma counter and expressed as the percentage of the total activity added to the cells.

2.4.4. Retention studies

After 2 h preincubation of cells with each ^{67}Ga complex in humidified 5% CO_2 atmosphere, at 37 °C, the medium containing the complex was removed, washed with cold PBS and replaced by fresh medium. The cellular retention of the internalized ^{67}Ga complex was determined up to 1 h by washing twice the cells with cold PBS, lysis with 0.1 M NaOH and measured of radioactivity.

Table 2
Cadherin expression in different cancer cell lines [11,43,44].

	A375[11]	PC-3[43]	MCF-7[44]	MDA-MB-231[44]
Cancer cell type	Melanoma	Prostate	Breast	Breast
N-Cadherin	+	+	–	–
E-Cadherin	–	+	+	–

2.4.5. Cytotoxicity assays

The cytotoxicity of the complexes against the MDA-MB-231 cells was evaluated using a colorimetric method based on the tetrazolium salt MTT (3-(4,5-dimethylthiazol-2-yl)-2,5-diphenyltetrazolium bromide), which is reduced by viable cells to yield purple formazan crystals. Cells were seeded in 96-well plates at a density of 0.8×10^4 cells per well in 200 μl of culture medium and left to incubate overnight for optimal adherence. After careful removal of the medium, 200 μL of a dilution series of the compounds (stock solutions prepared fresh; 200–0.1 μM) in medium were added and incubation was performed at 37 °C/5% CO_2 for 72 h. The percentage of DMSO in cell culture medium did not exceed 1%. At the end of the incubation period, the compounds were removed and the cells were incubated with 200 μl of MTT solution (500 μg/ml). After 3–4 h at 37 °C/5% CO_2, the medium was removed and the purple formazan crystals were dissolved in 200 μl of DMSO by shaking. The cell viability was evaluated by measurement of the absorbance at 570 nm using a plate spectrophotometer (Power Wave Xs, Bio-Tek). The cell viability was calculated dividing the absorbance of each well by that of the control wells. Each experiment was repeated at least two times and each point was determined in at least four replicates.

3. Results and discussion

3.1. Synthesis and characterization of the peptide and its conjugates

The pentapeptide HAVAY-NH_2 was synthesized by Fmoc solid phase peptide synthesis using a microwave-assisted peptide synthesizer and fully characterized by NMR spectroscopy, Mass Spectrometry and pH-potentiometry (see experimental part). The titration curve of the peptide (Fig. S1) indicates three deprotonation processes with p*K* values of 5.44(1), 7.27(2) and 9.52(3) (Table S1), which most likely belong to the imidazolium side chain, the N-terminal ammonium group and to the tyrosine phenolic OH-groups, respectively, in agreement with the structure of the peptide.

Conjugation of HAVAY-NH_2 to the metal fragment RuCp was accomplished using visible-light irradiation (see Scheme 1) as previously reported for aromatic side chain-containing amino acids [26] and monitored by ^{1}H NMR (Fig. 1). The spectra clearly show the appearance of new signals at 7.55 and 7.92 ppm attributed to free naphthalene, at 6.11 ppm assigned to Tyr and at 5.34 ppm for RuCp in a new chemical environment, strongly suggesting the formation of the full sandwich type complex (η^6-Tyr-RuCp)-HAVAY-NH_2, where the metal ion is

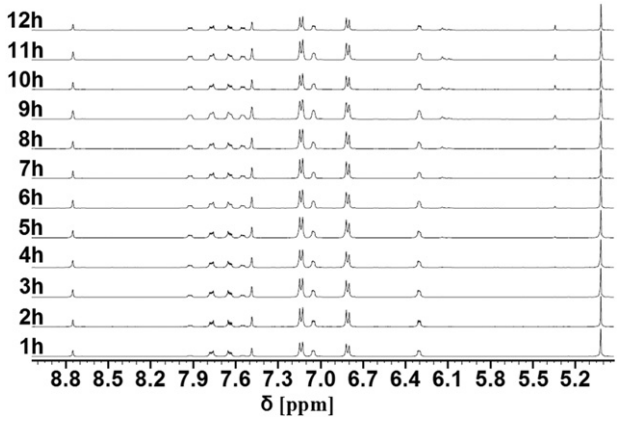

Fig. 1. Time dependence of the low-field region of the ^{1}H NMR spectrum of a sample containing HAVAY-NH_2 and [η^5-Cp(η^6-naphthalene)Ru]$^+$ in D_2O (T = 298.15 K).

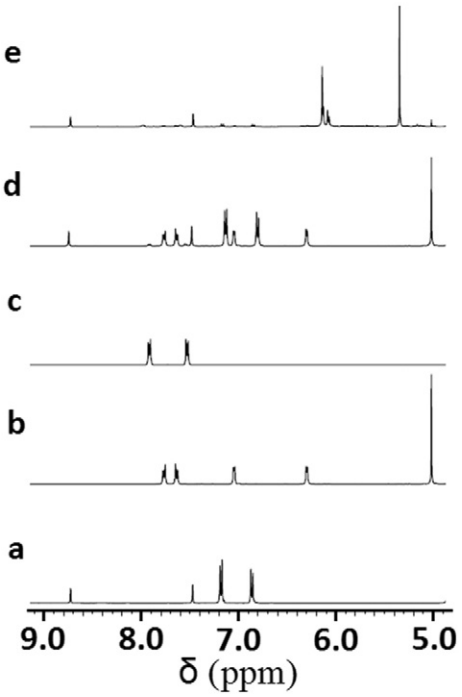

Fig. 2. Low-field region of the ^{1}H NMR spectra of HAVAY-NH_2 (a), [η^5-cyclopentadienyl(η^6-naphthalene)Ru]$^+$ (b), naphthalene (c) and that of the HAVAY-NH_2 – [η^5-cyclopentadienyl(η^6-naphthalene)Ru]$^+$ system in D_2O (T = 298.15 K) after 1 h (d) and 90 h (e) irradiation.

connected to the Tyr unit of the peptide. The reaction was found to be complete after four days as depicted in Fig. 2. Only the signals assigned to the Tyr of HAVAY-NH_2, but not those of the His amino acid, show a characteristic upfield shift (see Table 1). Furthermore, comparison of the resonance of the Cp signal (5.02 ppm) in the free complex [η^5-Cp(η^6-naphthalene)ruthenium(II)]$^+$ with the new resonance at 5.34 ppm is also consistent with the formation of the full sandwich type complex. Spectrum **e** in Fig. 2 shows the resonances of the complex after the removal of the free naphthalene as it was indicated in Part 2.2.2. Identical trend in the shift of the signal belonging to η^5-Cp*Rh^{2+} was observed upon the chemoselective coordination of Tyr^1 of Leu-enkephalin to this half-sandwich core [22]. ESI-MS spectrum provided (Fig. 3) corroborates for the formation and identity of the peptide complex. Indeed, the MS spectrum acquired in the reaction mixture

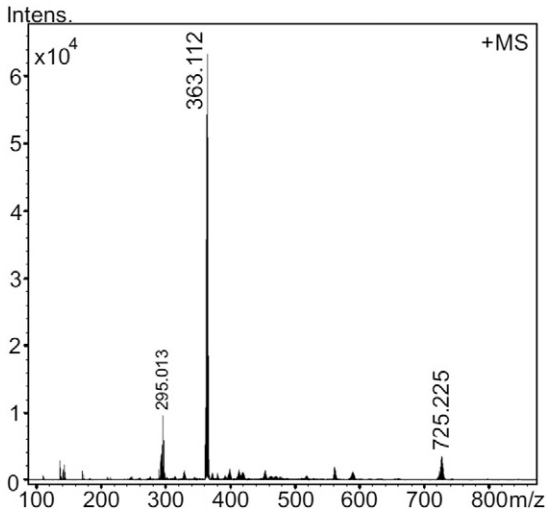

Fig. 3. ESI-TOF-MS spectrum of the [(η^5-cyclopentadienyl)Ru(η^6-naphthalene)]$^+$ – HAVAY-NH_2 system after 90 h visible-light irradiation.

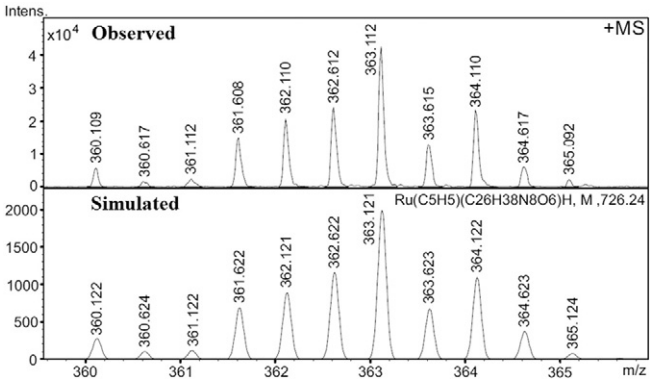

Fig. 4. Representative observed and simulated ESI-TOF-MS spectra of the full sandwich type [(η^6-Tyr-RuCp)-HAVAY-NH_2]$^{2+}$ complex.

supports the formation of the desired product, while in Fig. 4 the estimated and observed isotope pattern of [(η^6-Tyr-RuCp)-HAVAY-NH_2]$^{2+}$ can be seen.

As the resonances of the coordinated Tyr residue of HAVAY-NH_2 in Fig. 2e showed unexpected multiplicity we monitored whether light irradiation could also mediate the formation of the full sandwich (η^6-L-Tyr)Ru(η^5-Cp) complex with the model L-Tyr amino acid. For this, two samples (see experimental part 2.3.3.1 and 2.3.3.2) with either acidic or basic pH were prepared and characterized by NMR spectroscopy and Mass Spectrometry. In particular, the detailed pH dependence of the low-field region of the ^{1}H NMR spectrum of a mixture containing [η^5-Cp(η^6-naphthalene)ruthenium(II)]$^+$ and L-Tyr after 24 h visible-light irradiation is seen in Fig. 5. At pH 3.35, besides the two doublets of the free L-Tyr in the range 6.9–7.2 ppm the signal assigned to the complexed Tyr (6.0–6.2 ppm) and Cp (5.34 ppm) and uncomplexed RuCp precursor (5.02 ppm) are detected. As expected, on increasing the pH, the free L-Tyr signals show an upfield shift above pH 9.0 only, indicating the deprotonation of the phenolic OH while the Cp signal of the [η^5-Cp(η^6-naphthalene)ruthenium(II)]$^+$ at 5.02 ppm does not shift in the pH range studied. The resonances of complexed L-Tyr and Cp, however, exhibit an upfield shift with increasing pH, with the L-Tyr signals also splitting. The cross peak in the ^{1}H–^{1}H COSY spectrum (Fig. 2S) at pH = 9.73 between the resonances at 5.50 and 5.77 ppm supports the fact that these signals belong to protons in a non-symmetrical environment of the same phenyl ring. The ^{1}H–^{13}C HSQC spectrum (Fig. 3S) also

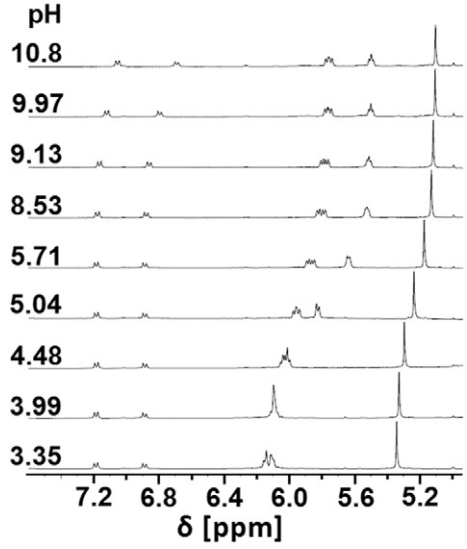

Fig. 5. Dependence on pH of the low-field region of the NMR spectra of a mixture containing [η^5-Cp(η^6-naphthalene)ruthenium(II)]$^+$ and L-Tyr in D_2O after 24 h visible-light irradiation.

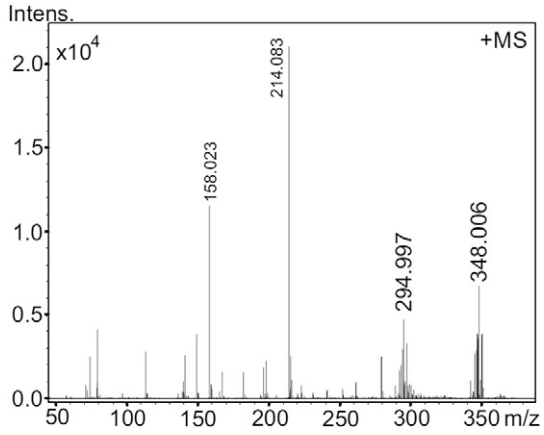

Fig. 6. ESI-MS spectrum of a solution containing $[\eta^5$-Cp(η^6-naphthalene)ruthenium(II)$]^+$ and L-Tyr at 1:1 ratio after 24 h visible-light irradiation at pH = 2.02.

provides proof for this. Furthermore, this multiplicity change of the resonances of the Tyr ring protons can be rationalized with the change in hapticity from η^6 to η^5 (oxohexadienyl coordination) if the pH is increased. Evaluation of the pH-dependent shift (Fig. 5) of the complexed L-Tyr (two multiplets) and Cp signals by the Scientist program [42] resulted in p*K* values of 5.09(11), 5.08(3) and 5.11(7), respectively, which clearly indicate that all these signals belong to the same molecule revealing thus the formation of the full sandwich structure. Identical increase in the acidity of the phenolic OH-group of L-Tyr upon coordination in a full sandwich complex and change in hapticity was also reported for (η^6-*p*-cym)Ru(η^6-Tyr) or (η^5-Cp*)Rh/Ir(η^6-Tyr) [31,32,45–47]. MS information (Fig. 6) at various pH values is also consistent with the formation of the above mentioned complex and as a representative example the excellent agreement of the estimated and observed spectra are shown in Fig. S4.

The peptide-containing complex $[(\eta^6$-Tyr-RuCp)-HAVAY-$NH_2]^{2+}$ was reacted with NODA-GA in DIPEA/DMF with formation of thiourea bonds between the bifunctional chelator and the terminal amino group, leaving all three carboxylic groups of the macrocycle intact and available for coordination to Ga(III) [48]. The same reaction was also carried out using HAVAY-NH_2 for comparative purposes. The conjugates obtained were purified by semi-preparative HPLC (*system III*). After lyophilisation, the identity of the compounds was checked by Mass Spectrometry and ^{1}H NMR spectroscopy. Representative ESI-MS spectra (see Figs. S5, S6 and S7) show the observed m/z values.

Reaction of the NODA-containing compounds with $Ga(NO_3)_3 \cdot H_2O$ afforded the corresponding gallium(III) complexes, [Ga-NODA-GA-HAVAY-NH_2](CH_3COO) and [Ga-NODA-GA-(η^6-Tyr-RuCp)-HAVAY-NH_2]($CH_3COO)_2$. These complexes were purified by HPLC (*system III*) and their identity was confirmed by ^{71}Ga NMR spectroscopy and ESI-MS (Figs. S8 and S9). pH dependence of equilibrated samples with $Ga(NO_3)_3$ and the NODA-containing compounds revealed the formation of the corresponding complex (Fig. S8) as the signal of ^{71}Ga showed a significant downfield shift upon complexation (0 ppm $[(Ga(H_2O)_6]^{3+}$; 164.7 ppm Ga-NODA-GA-HAVAY-NH_2, 164.5 ppm Ga-NODA-GA-[(η^6-Tyr-RuCp)-HAVAY-NH_2]; T = 313.15 K), and the chemical shift value is in the range of values for similar Ga(III)-macrocycle complexes (NOTA: 171, NOTAC6: 165.5 and NOTAC8: 165.8 ppm) [33]. As a further proof, the obtained T_1 = 4.399(10) ms relaxation time for the [Ga-NODA-GA-HAVAY-NH_2](CH_3COO) complex also supports the conformity with an octahedral coordination what has been observed for $[Ga(H_2O)_6]^{3+}$ (T_1 = 5.529(1) ms) at the same temperature, T = 313.15 K. The ^{71}Ga NMR signal was observed unchanged over a period of a month, reflecting the high stability of the chelate in aqueous solution.

Radiolabelling of the above NODA-containing compounds with ^{67}Ga was carried out in acetate buffer by reacting the NODA-containing compounds with the radioactive precursor $^{67}GaCl_3$ at room temperature for 1 h. The resulting complexes [^{67}Ga-NODA-GA-HAVAY-NH_2](CH_3COO) and [^{67}Ga-NODA-GA-(η^6-Tyr-RuCp)-HAVAY-NH_2]($CH_3COO)_2$ were

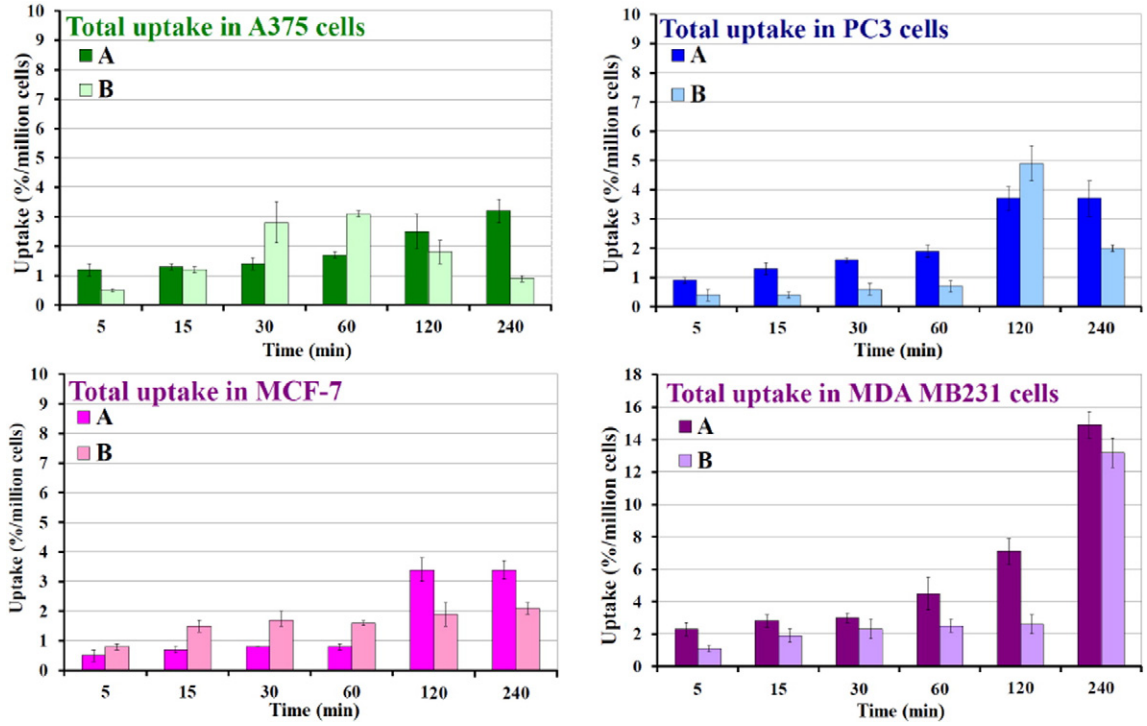

Fig. 7. Cellular uptake of ^{67}Ga-NODA-GA-HAVAY-NH_2 (A) and ^{67}Ga-NODA-GA-(η^6-Tyr-RuCp)-HAVAY-NH_2 (B) in human cancer A375, PC-3, MCF-7 and MDA-MB-231 cells expressed as a percentage of total radioactivity per million cells.

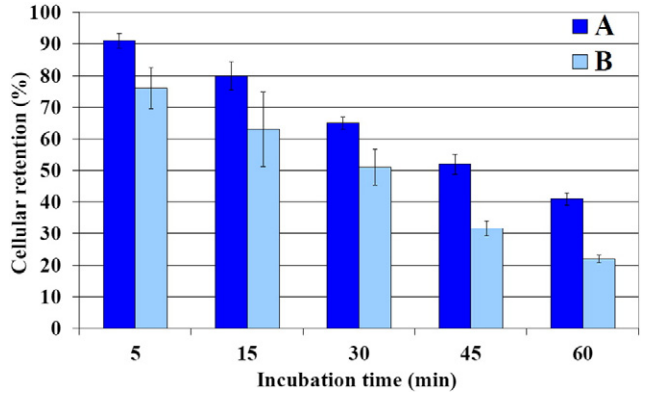

Fig. 8. Cellular retention of internalized ^{67}Ga-NODA-GA-HAVAY-NH_2 (A) and ^{67}Ga-NODA-GA-(η^6-Tyr-RuCp)-HAVAY-NH_2 (B) in MDA-MB-231 cells over time.

purified by a Sep-pak C18 cartridge and obtained with high radiochemical purity (>95%) as confirmed by HPLC analysis (*system IV*). The fractions collected were used for the various biological studies described below.

3.2. Cellular uptake studies

The cellular uptake of the ^{67}Ga-compounds was studied in four human cancer cell lines, MCF-7, MDA-MB-231 (breast), A375 (melanoma) and PC-3 (prostate) (Table 2) up to 4 h. In general, the results indicate (Fig. 7) a moderate uptake in the four lines that increases over time. The highest uptake was found in breast MDA-MB-231 cells (14.9 ± 0.8% and 13.2 ± 0.9% for [^{67}Ga-NODA-GA-HAVAY-NH_2](CH_3COO) (**A**) and [^{67}Ga-NODA-GA-(η^6-Tyr-RuCp)-HAVAY-NH_2](CH_3COO)$_2$ (**B**), respectively, at 4 h). This trend seems to be in good agreement with the highest cytotoxicity of the [^{nat}Ga-NODA-GA-HAVAY-NH_2](CH_3COO) complex, whose results are also presented hereafter.

The internalization of the ^{67}Ga complexes and the radioactivity associated to the cell membrane was also evaluated in the same cell lines (data not shown), however, the internalization is very low in any of the cell lines (<0.7%/million cells) while a considerable amount of radioactivity remains associated to the cell membrane (reaching 6–7%/million cells). This finding may explain the low cytotoxic activity of the cold Ga complexes described below. Additionally to the low rate of internalization a low cellular retention was observed with 41% and 22% of the internalized activity retained into the cells after 1 h (Fig. 8).

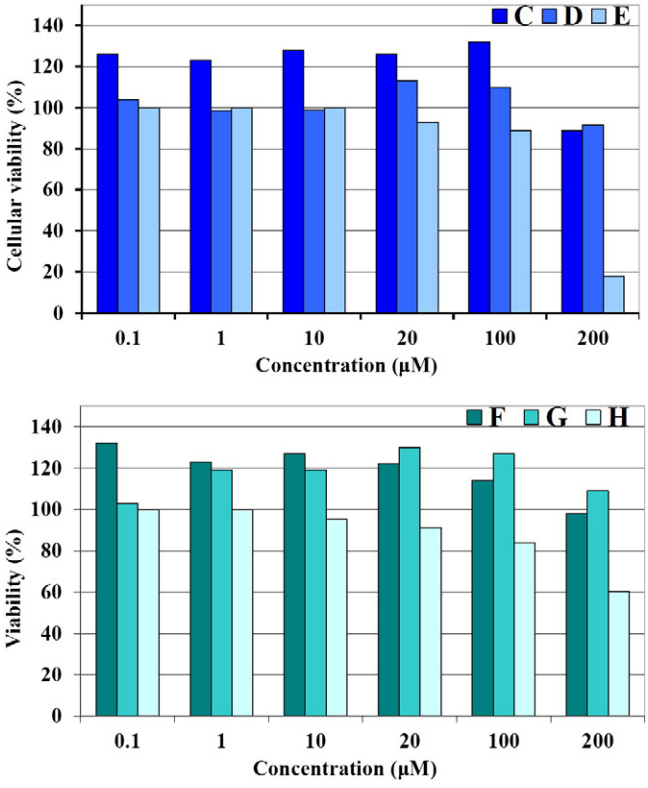

Fig. 9. Cellular viability of MDA-MB-231 cells treated with HAVAY-NH_2 (C), NODA-GA-HAVAY-NH_2 (D), Ga-NODA-GA-HAVAY-NH_2 (E), (η^6-Tyr-RuCp)-HAVAY-NH_2 (F), NODA-GA-(η^6-Tyr-RuCp)-HAVAY-NH_2 (G) and Ga-NODA-GA-(η^6-Tyr-RuCp)-HAVAY-NH_2 (H) for 72 h at 37 °C.

3.3. MTT viability assay

The cytotoxic activity of HAVAY-NH_2 (**C**), NODA-GA-HAVAY-NH_2 (**D**), Ga-NODA-GA-HAVAY-NH_2 (**E**), (η^6-Tyr-RuCp)-HAVAY-NH_2 (**F**), NODA-GA-(η^6-Tyr-RuCp)-HAVAY-NH_2 (**G**) and Ga-NODA-GA-(η^6-Tyr-RuCp)-HAVAY-NH_2 (**H**) was tested on human breast cancer MDA-MB-231 cells. These cells were treated with decreasing concentrations (200–0.1 μM) of the each compound and incubated for 72 h at 37 °C. All tested compounds were solubilized in water and then diluted in the cell culture medium. After appropriate treatment, the cellular viability was assessed by the MTT assay. The inhibition of growth was calculated by correlation with vehicle treated cells. Results are presented as percentage of viable cells (Fig. 9).

The results obtained indicated that in general none of the ligands (HAVAY-NH_2, (η^6-Tyr-RuCp)-HAVAY-NH_2 and respective NODA-GA conjugates) exhibited any cytotoxicity. Nevertheless, the Ga complexes inhibited cell growth, for concentrations above 100 μM, especially the Ga-NODA-GA-HAVAY-NH_2 complex. However, that inhibition is not significant.

4. Conclusions

We have synthesized and fully characterized, to the best of our knowledge, the first heterobimetallic complexes containing a histidyl-alanyl-valinyl (HAV) sequence for targeting, a full sandwich Ru(II) unit with potential anticancer activity and a ^{nat}Ga- or ^{67}Ga-NODA-GA moiety to monitor biodistribution. The cellular uptake of the ^{67}Ga-compounds was studied in four human cancer cell lines, and a low to moderate uptake was observed. The highest uptake was found in breast MDA-MB-231 cells. The internalization of the ^{67}Ga complexes was also very low in any of the cell lines tested while a considerable amount of radioactivity remained associated to the cell membrane. Additionally to the low rate of internalization a low cellular retention was also observed. Brought together, these cell assays may explain the low cytotoxic activity associated to the non-radioactive ^{nat}Ga complexes.

Abbreviations

AcOH	acetic acid
A375	human malignant melanoma cell line
BSA	bovine serum albumin
Cadherin	Calcium-dependent cell adhesion protein
CAR	cell adhesion recognition
COSY	Correlation Spectroscopy
Cp	cyclopentadienyl anion
Cp*	pentamethylcyclopentadienyl anion
DCM	dichloromethane
DIPEA	N,N-diisopropyl-ethylamine
DMF	N,N-dimethylformamide
DMSO	dimethyl sulfoxide, $(CH_3)_2SO$
DODT	3,6-dioxa-1,8-octanedithiol
ESI-TOF-MS	ElectroSpray Ionization Time-Of-Flight Mass Spectrometry
Fmoc	N-fluorenylmethoxycarbonyl

HAV histidyl-alanyl-valinyl sequence, His-Ala-Val
HAVAY-NH_2 H-His-Ala-Val-Ala-Tyr-NH_2
HOBt·H_2O 1-hydroxybenzotriazole hydrate
HSQC Heteronuclear Single Quantum Coherence
MCF-7 hormone-dependent human breast adenocarcinoma cell line
MDA-MB-231 hormone-independent human breast adenocarcinoma cell line
MTT 3-(4,5-dimethylthiazol-2-yl)-2,5-diphenyltetrazolium bromide
^{nat}Ga natural, stable isotopes of gallium
NMP N-methylpyrrolidone
NODA-GA 2,2′-(7-(1-carboxy-4-((4-isothiocyanatobenzyl)amino)-4-oxobutyl)-1,4,7-triazonane-1,4-diyl)diacetic acid
NOTA 1,4,7-triazacyclononane-1,4,7-triacetic acid
NOTAC6 1,4,7-triazacyclononane-1-hexanoic acid-4,7-diacetic acid
NOTAC8 1,4,7-triazacyclononane-1-octanoic acid-4,7-diacetic acid
PBS phosphate-buffer saline
PC-3 human prostate adenocarcinoma cell line
p-cym 1-methyl-4-isopropylbenzene
RuCp [(η^5-cyclopentadienyl)Ru]$^+$, [(η^5-C_5H_5)Ru]$^+$
TBTU 2-(1-H-benzotriazole-1-yl)-1,1,3,3-tetramethyluronium tetrafluoroborate
TFA trifluoroacetic acid
TIS triisopropylsilane
Tyr L-Tyrosine
[(η^6-Tyr-RuCp)-HAVAY-NH_2] H-His-Ala-Val-Ala-(η^6-Tyr-RuCp)-NH_2
^{67}Ga Gallium-67 is a gamma-emitting isotope with $t_{1/2} = 3.26$ days

Acknowledgments

The authors thank members of the EU COST Action CM1105 for motivating discussions. The research was supported by an EU COST Action CM1105 STSM, Hungarian Scientific Research Fund (OTKA K112317) and the Richter Gedeon Talentum Foundation. C^{2}TN/IST authors gratefully acknowledge the support of the Fundação para a Ciência e Tecnologia through the projects UID/Multi/04349/2013 and EXCL/QEQ-MED/0233/2012. We thank Dr. Zsolt Baranyai for his help in acquiring the ^{71}Ga NMR spectra.

Appendix A. Supplementary data

Supplementary data to this article can be found online at http://dx.doi.org/10.1016/j.jinorgbio.2016.02.011.

References

[1] Y.-R. Zheng, K. Suntharalingam, T.C. Johnstone, S.J. Lippard, Chem. Sci. 6 (2015) 1189–1193.
[2] J.D.G. Correia, A. Paulo, P.D. Raposinho, I. Santos, Dalton Trans. 40 (2011) 6144–6167.
[3] N. Metzler-Nolte, in: G. Jaouen (Ed.), Bioorganometallics, Wiley-VCH, Weinheim, Germany 2006, pp. 125–179.
[4] T. Kammertoens, T. Schüler, T. Blankenstein, Trends Mol. Med. 11 (2005) 225–231.
[5] V. Noë, J. Williams, J. Vandekerckhove, F.V. Roy, E. Bruyneel, M. Mareel, J. Cell Sci. 112 (1999) 127–135.
[6] M. Takeichi, Science 251 (1991) 1451–1455.
[7] O.W. Blaschuk, E. Devemy, Eur. J. Pharmacol. 625 (2009) 195–198.
[8] O.W. Blaschuk, Philos. Trans. R. Soc. B 370 (2015) 20140039.
[9] J. Folkman, Nat. Rev. Drug Discov. 6 (2007) 273–286.
[10] N. Yarom, D. Stewart, L. Avruch, R. Malik, J. Wells, D.J. Jonker, Anticancer Res. 31 (2011) 3921–3926.
[11] C.K. Augustine, Y. Yoshimoto, M. Gupta, P.A. Zipfel, M.A. Selim, P. Febbo, A.M. Pendergast, W.P. Peters, D.S. Tyler, Cancer Res. 68 (10) (2008) 3777–3784.
[12] N. Kobayashi, A. Ikesue, S. Majumdar, T.J. Siahaan, J. Pharmacol. Exp. Ther. 317 (2006) 309–316.
[13] N.H. On, P. Kiptoo, T.J. Siahaan, D.W. Miller, Mol. Pharmacol. 11 (2014) 974–981.
[14] M. Melchart, P.J. Sadler, in: G. Jaouen (Ed.), Bioorganometallics, Wiley-VCH, Weinheim, Germany 2006, pp. 39–64.
[15] I. Bratsos, T. Gianferrara, E. Alessio, C.G. Hartinger, M.A. Jakupec, B.K. Keppler, in: E. Alessio (Ed.), Bioinorganic Medicinal Chemistry, Wiley-VCH, Weinheim, Germany 2011, pp. 160–164.
[16] G. Süss-Fink, Dalton Trans. 39 (2010) 1673–1688.
[17] A. Gross, N. Metzler-Nolte, J. Organomet. Chem. 694 (2009) 1185–1188.
[18] B.T. Loughrey, P.C. Healy, P.G. Parsons, M.L. Williams, Inorg. Chem. 47 (2008) 8589–8591.
[19] B.T. Loughrey, B.V. Cunning, P.C. Healy, C.L. Brown, P.G. Parsons, M.L. Williams, Chem. Asian. J. 7 (2012) 112–121.
[20] F. Baragán, P. Lopez-Shenín, L. Shalassa, S. Betanzos-Lara, A. Haptemariam, V. Moreno, P.J. Sadler, V. Marchán, J. Am. Chem. Soc. 133 (2011) 14098.
[21] J. Lempke, N. Metzler-Nolte, J. Organomet. Chem. 696 (2011) 1018.
[22] H.B. Albada, F. Wieberneit, I. Dijkgraaf, J.H. Harvey, J.L. Whistler, R. Stoll, N. Metzler-Nolte, R.H. Fish, J. Am. Chem. Soc. 134 (2012) 10321–10324.
[23] D.B. Grotjahn, C. Joubran, D. Combs, D.C. Brune, J. Am. Chem. Soc. 120 (1998) 11814.
[24] D.B. Grotjahn, Coord. Chem. Rev. 190-192 (1999) 1125.
[25] D.S. Perekalin, A.P. Molotkov, Y.V. Nelyubina, N.Y. Anisimova, A.R. Kudinov, Inorg. Chim. Acta 409 (2014) 390–393.
[26] D.S. Perekalin, E.E. Karslyan, P.V. Petrovskii, Y.V. Nelyubina, K.A. Lyssenko, A.S. Kononikhin, E.N. Nikolaev, A.R. Kudinov, Chem. Eur. J. 16 (2010) 8466–8470.
[27] R. Krämer, Angew. Chem. Int. Ed. Engl. 35 (1996) 1197–1199.
[28] D.S. Perekalin, V.V. Novikov, A.A. Pavlov, I.A. Ivanov, N.Y. Anisimova, A.N. Kopylov, D.S. Volkov, I.F. Deregina, M.A. Bolshov, A.R. Kudinov, Chem. Eur. J. 21 (2015) 4923–4925.
[29] D.S. Perekalin, A.R. Kudinov, Coord. Chem. Rev. 276 (2014) 153–173.
[30] R.M. Moriarty, Y.-Y. Ku, U.S. Gill, J. Chem. Soc., Chem. Commun. (1987) 1837–1838.
[31] W.S. Sheldrick, A. Gleichmann, J. Organomet. Chem. 470 (1994) 183–187.
[32] D.A. Herebian, C.S. Shmidt, W.S. Sheldrick, C. van Wüllen, Eur. J. Inorg. Chem. (1998) 1991–1998.
[33] H.R. Maecke, M. Hofmann, U. Haberkorn, J. Nucl. Med. 46 (2005) 172S–178S.
[34] A. de Sá, M.I.M. Prata, C.F.G.C. Geraldes, J.P. André, J. Inorg. Biochem. 104 (2010) 1051–1062.
[35] M. Morais, C. Cantante, L. Gano, I. Santos, S. Lourenço, C. Santos, C. Fontes, F. Aires da Silva, J. Gonçalves, J.D.G. Correia, Nucl. Med. Biol. 41 (2014) 44–48.
[36] A. de Sá, Á.A. Matias, M.I.M. Prata, C.F.G.C. Geraldes, P.M.T. Ferreira, J.P. André, Bioorg. Med. Chem. Lett. 20 (2010) 7345–7348.
[37] V. Scasnar, J.E. Vanlier, Eur. J. Nucl. Med. 20 (1993) 273.
[38] G. Gran, Acta Chem. Scand. 4 (1950) 559–577.
[39] H.M. Irving, M.G. Miles, L.D. Pettit, Anal. Chim. Acta 38 (1967) 475–488.
[40] P. Gans, A. Sabatini, A. Vacca, J. Chem. Soc. Dalton Trans. (1985) 1195–1200.
[41] A. Krezel, W. Bal, J. Inorg. Biochem. 98 (2004) 161–166.
[42] Micromath Scientist, v. 2.01, MicroMath Inc., Salt Lake City, UT, USA, 1995.
[43] N.L. Tran, R.B. Nagle, A.E. Cress, R.L. Heimark, Am. J. Pathol. 155 (1999) 787–798.
[44] M.T. Nieman, R.S. Prudoff, K.R. Johnson, M.J. Wheelock, J. Cell Biol. 147 (1999) 631–644.
[45] B. Chaudret, X. He, Y. Huang, J. Chem. Soc. Chem. Commun. (1989) 1844–1846.
[46] U. Koelle, M.H. Wang, G. Raabe, Organometallics 10 (1991) 2573–2577.
[47] J.M. Wolff, W.S. Sheldrick, Chem. Ber. /Recueil 130 (1997) 981–988.
[48] L. Land, Y. Ma, D.O. Kiesewetter, X. Chen, Mol. Pharm. 11 (2014) 3867–3874.